



OPEN Dual acid-base catalysis with biologically modified graphene oxide: a sustainable route to polyhydroquinolines with antimicrobial properties

Leila Amiri-Zirtol¹, Hamideh Emtiazi², Seyedeh Narjes Abootalebi^{1,3}✉ & Ahmad Gholami^{1,4}✉

This article conducts an in-depth examination of graphene oxide-aspartic acid (GO-As) as a novel bifunctional nano-organocatalyst distinguished by both catalytic and antibacterial properties. The research elucidates the synthesis of GO through Hummer's method, followed by the covalent attachment of aspartic acid to the surface of GO nanosheets. This innovative approach is particularly notable as it circumvents the use of hazardous chemicals, thereby promoting environmental sustainability. The newly developed catalyst underwent rigorous analysis employing a variety of spectroscopic techniques, including Fourier Transform Infrared (FT-IR) spectroscopy, Energy-Dispersive X-ray Spectroscopy (EDX), mapping, Field Emission Scanning Electron Microscopy (SEM), X-ray diffraction (XRD), thermogravimetric analysis (TGA), and Raman spectroscopy. The findings indicate that the catalyst effectively synthesizes polyhydroquinoline derivatives while demonstrating significant stability over multiple reuse cycles, underscoring its potential applicability in organic synthesis. Furthermore, the antibacterial properties of the GO-modified aspartic acid were evaluated against six pathogenic bacterial species. The results reveal substantial antibacterial activity against both Gram-positive and Gram-negative strains, including two antibiotic-resistant bacteria: Methicillin-resistant *Staphylococcus aureus* (MRSA), Vancomycin-resistant *Enterococcus* (VRE), thermogravimetric analysis (TGA), and Raman. In conclusion, the investigation of GO-As as a bifunctional heterogeneous nano-organocatalyst represents a promising advancement in the development of environmentally friendly and effective catalysts with noteworthy antibacterial characteristics.

Keywords Green chemistry, Functionalized graphene oxide, Aspartic acid-based nanocomposite, Antimicrobial activity

Abbreviations

FT-IR	Fourier transform infrared
XRD	X-ray diffraction
EDX	Energy-dispersive X-ray
FE-SEM	Field emission scanning electron microscope
TLC	Thin layer chromatography
EtOH	Ethanol
GO	Graphene oxide
As and ASP	aspartic acid
GO-As and GO-ASP	Graphene oxide-aspartic acid

¹Biotechnology Research Center, Shiraz University of Medical Sciences, Shiraz, Iran. ²Faculty of Pharmacy, Shahid Sadoughi University of Medical Sciences, Yazd, Iran. ³Division of Intensive Care Unit, Department of Pediatrics, School of Medicine, Shiraz University of Medical Sciences, Shiraz, Iran. ⁴Department of Pharmaceutical Biotechnology, School of Pharmacy, Shiraz University of Medical Sciences, Shiraz, Iran. ✉email: Abootalebinarjes@yahoo.com; Gholami@sums.ac.ir

Green chemistry focuses on designing chemical products and processes to reduce hazardous substances. Recent decades have strongly emphasized conducting reactions sustainably, with metal-free reactions gaining importance for their environmental benefits^{1–3}. Organocatalysts play a key role in aligning with these green chemistry principles. Organocatalysts are gaining attention in organic compound synthesis because of their advantages: availability, reusability, nontoxicity, biocompatibility, and cost-effectiveness^{4,5}. For example, magnetic guanidinylation chitosan has been used as a magnetic organocatalyst to synthesize certain heterocyclic compounds⁶.

Amino acids are effective and cost-efficient biological organocatalysts due to their acidic and basic functional groups⁷. In 2017, Tiwari et al. synthesized 2-amino-3-cyano-4-H-pyrans using valine as a catalyst⁸. Later, in 2020, Amirnejat et al. developed an alginate-based nanocomposite catalyst for imidazole synthesis, enhanced with arginine and Fe₃O₄⁹. However, this approach faced issues with toxic chemicals and high production costs. Aspartic acid (As) is a natural amino acid featuring two carboxyl groups, one on the alpha carbon and another on the side chain^{10,11}. It plays a role in protein biosynthesis and is also used to synthesize various organic compounds, including tetrahydrobenzo[b]pyrans, tetrasubstituted imidazoles, 2-amino-4 H-chromene, 2-amino-3-cyano-4 H-pyrans, 1 H-pyrano[2,3-d] pyrimidine-2, 4(3 H,5 H)-diones, and 1,4-dihydropyrano[2,3-c] pyrazoles^{12–14}. While organocatalysts offer advantages, their free forms struggle with reusability and separation. Stabilizing them on substrates like graphene oxide (GO) presents a promising solution due to GO's simple synthesis, two-dimensional structure, and versatile functional groups^{15,16}. Modifying GO can increase its applicability in polymer grafting and composite materials, especially by activating carboxylic groups for amide formation and coupling with octadecylamine^{17–19}.

the MCR reaction of aldehydes, ethyl acetoacetate, and ammonia. Multicomponent reactions (MCRs) offer straightforward, effective, and practical approaches in contemporary medicinal and combinatorial chemistry^{20–22}. 1,4-Dihydropyridines (1,4-DHPs) and polyhydroquinolines (PHQs) are nitrogen-containing heterocyclic compounds recognized for their diverse biological activities, which include neurotropic, anticancer, antibacterial, and antiproliferative properties^{23,24}. These compounds present significant advantages, such as a straightforward design and high atom economy^{25–30}. Nevertheless, existing synthetic methodologies often face considerable challenges. These methods frequently utilize catalysts, including acidic ionic liquids and metal nanoparticles, which may result in extended reaction times, reliance on organic solvents, and complex procedural requirements^{31–33}. For example, Dekamin et al. explored the use of alginic acid as a catalyst; however, this approach yielded low results over prolonged reaction periods³⁴. Similarly, Amiri et al. utilized 4-(2-Aminoethyl)-morpholine in conjunction with Fe₃O₄@SiO₂, a method characterized by a cumbersome and costly synthesis process⁵. This situation underscores the need to develop more efficient and environmentally benign catalytic methodologies. Therefore, in continuation of our research to develop better synthetic methods for synthesizing polyhydroquinolines, we introduced aspartic acid immobilized on the surface of GO nanosheets as a heterogeneous natural biocatalyst with dual acidic and basic properties.

This study presents an innovative method for synthesizing a catalyst by stabilizing as on graphene oxide through covalent bonding. This approach yields composite materials incorporating natural amino acids, exhibiting catalytic and antibacterial properties. The advantages of this method include a straightforward and safe synthesis process, ease of recovery, and the capability of the catalysts to be reused while maintaining efficiency across multiple reactions. Our process promptly facilitates high product yields, utilizing green solvents and mild reaction conditions. The methodology entails a nucleophilic attack by the amino group (NH₂) on the epoxide rings of graphene oxide, resulting in the formation of a covalent bond while preserving the carboxylic acid groups (COOH) that enhance acidity. In contrast to alternative methods that rely on harmful chemicals, our functionalization is conducted under environmentally benign conditions, employing water as the solvent and maintaining ambient temperature, thereby aligning with the principles of green chemistry.

Developing new antimicrobial agents is essential due to the urgent need to create new classes of antimicrobial compounds that possess novel modes of action capable of overcoming the resistance mechanisms seen in conventional antibiotics^{35,36}. Recent studies have demonstrated the antimicrobial activity of amino acids in larger, more complex proteins and short-chain peptides^{37,38}. In light of this, the antibacterial activity of the nanocomposite developed in this study was evaluated against four strains of bacteria: *Escherichia coli* (*E. coli*), *Staphylococcus aureus* (*S. aureus*), *Salmonella typhimurium* (*S. typhi*), and *Enterococcus faecalis* (*E. faecalis*), as well as two antibiotic-resistant strains, methicillin-resistant staphylococcus aureus (MRSA) and vancomycin-resistant enterococcus (VRE).

Experimental

Materials and methods

All the solvents, reagents, and chemical powders used in this work were purchased from Merck Chemical Co. (Germany) and Aldrich and used without purification. Scanning electron micrograph (SEM) was provided on a VEGA-TESCAN. The X-ray diffraction (XRD) patterns of the solid powders were recorded using an X' Pert Pro X-ray diffractometer, operated at 40 mA and 40 kV, to ensure accurate and reliable data for analysis. An energy-dispersive X-ray spectroscopy (EDS) study was performed using Zeiss SIGMA VP-500. The spectral data, including ¹H NMR, ¹³C NMR, and IR, for compounds 3, 5, 7, and 8 are provided in the supplementary section.

Synthesis of graphene oxide-aspartic acid (GO-AS)

To create the graphene oxide-aspartic acid nanocomposite, graphene oxide first had to be made using the previous methods³⁹. Then, in a 100 ml flask, graphene oxide powder (5.5 g) was dispersed in 30 ml of water for 20 min. Next, 5.5 g of K₂CO₃ and 5.5 g of aspartic acid were added to the reaction container, and the reaction

mixture was stirred for 24 h at room temperature. The composite was separated by filtration, washed in hot water/ethanol solvent, and dried at room temperature for 48 h. (Fig. 1)

Synthesis of polyhydroquinolines

Using GO-As (0.03 g) as a catalyst in a water/ethanol solvent and at 70 °C, a combination of aldehyde (1 mmol), ethyl acetoacetate (0.13 g, 1 mmol), dimedone (0.14 g, 1 mmol), and NH_4OAc (0.115 g, 1.2 mmol) was agitated in a 50 mL round-bottom flask fitted with a magnetic bar. The reaction was allowed to be completed, and TLC monitored its progress. After the completion of the reaction, the catalyst was separated from the reaction mixture by filtration, and the reaction solvent was removed. The obtained residue was recrystallized, and the PHQ product was purified in ethanol solvent and dried at 60 °C in an oven for 1 h.

Selected data

*Ethyl 4-(3-hydroxyphenyl)-2,7,7-trimethyl-5-oxo-1,4,5,6,7,8-hexahydroquinoline-3-carboxylate*³

Yellow solid, M.P.: 208–209 °C, IR (KBr) ν (cm^{-1}): 3281 (OH, N-H), 3077 (C-H, aromatic), 2960 (C-H, aliphatic), 1666 (C=O ester), 1611 (C=O), 1484 (C=C, aromatic), 1309 (C-O), 1286 (C-O, ether). ^1H NMR (400 MHz, $\text{DMSO}-d_6$): δ (ppm) = 0.81 (s, 3 H, CH_3), 0.98 (s, 3 H, CH_3), 1.09 (t, 3 H, $\text{O}-\text{CH}_2-\text{CH}_3$), 1.95 (d, 1H, CH), 2.14 (d, 1H, CH), 2.25 (m, 1H, CH), 2.27 (s, 3 H, CH_3), 2.39 (d, 1H, CH), 3.43 (q, 2 H, $\text{O}-\text{CH}_2-\text{CH}_3$), 4.74 (s, 1H, CH), 6.57 (d, 2 H, Ar-H), 6.95 (m, 1H), 8.99 (s, 1H), 9.07 (s, 1H, NH). ^{13}C NMR (100 MHz, $\text{DMSO}-d_6$): δ (ppm) 14.6, 18.7, 26.91, 29.64, 32.58, 35.25, 50.79, 59.42, 104.59, 110.7, 114.9, 128.8, 138.89, 144.85, 149.6, 155.7, 167.4, 194.8.

*Ethyl 4-(4-(dimethylamino)phenyl)-2,7,7-trimethyl-5-oxo-1,4,5,6,7,8-hexahydroquinoline-3-carboxylate*⁵

Yellow solid, M.P.: 232–234 °C, IR (KBr) ν (cm^{-1}): 3275 (N-H), 3074 (C-H, aromatic), 2958 (C-H, aliphatic), 1684 (C=O), 1606 (C=O), 1485 (C=C, aromatic), 1380 (C-O), 1277 (C-N). ^1H NMR (400 MHz, $\text{DMSO}-d_6$): δ (ppm) = 0.82 (s, 3 H, CH_3), 1.00 (s, 3 H, CH_3), 1.15 (t, 3 H, $\text{O}-\text{CH}_2-\text{CH}_3$), 1.98 (d, 1H, CH_2), 2.19 (d, 1H, CH_2), 2.25 (d, 1H, CH_2), 2.29 (s, 3 H, CH_3), 2.50 (d, 1H, CH_2), 2.79 (s, 6 H, 2 CH_3), 3.96 (q, 2 H, $\text{O}-\text{CH}_2-\text{CH}_3$), 4.72 (s, 1H, CH), 6.55 (d, 2 H, Ar-H), 6.96 (d, 2 H, Ar-H), 8.96 (s, 1H, NH). ^{13}C NMR (100 MHz, $\text{DMSO}-d_6$): δ (ppm) 14.67, 18.71, 27, 29.65, 32.59, 35.01, 50.78, 59.4, 104.7, 110.8, 112.4, 128.4, 136.5, 144.5, 149.13, 149.52, 167.56, 194.78.

*Ethyl 4-(4-methoxyphenyl)-2,7,7-trimethyl-5-oxo-1,4,5,6,7,8-hexahydroquinoline-3-carboxylate*⁷

Yellow solid, M.P.: 260–261 °C, IR (KBr) ν (cm^{-1}): 3199 (N-H), 3077 (C-H, aromatic), 2966 (C-H, aliphatic), 1701 (C=O), 1602 (C=O ketone), 1492 (C=C, aromatic), 1378 (C-O). ^1H NMR (400 MHz, $\text{DMSO}-d_6$): δ (ppm) = 0.85 (s, 3 H, CH_3), 1.13 (s, 3 H, CH_3), 1.16 (t, CH_3), 1.99 (d, 1H, CH_2), 2.19 (d, 1H, CH_2), 2.27 (s, 3 H, CH_3), 2.30 (d, 1H, CH_2), 2.44 (d, 1H, CH_2), 3.66 (s, 3 H, CH_3), 3.95 (q, $\text{O}-\text{CH}_2-\text{CH}_3$), 4.78 (s, 1H, CH), 6.75 (d, 2 H, Ar), 7.05 (d, 2 H, Ar), 9.03 (s, 1H, NH).

*Ethyl 4-(3-bromophenyl)-2,7,7-trimethyl-5-oxo-1,4,5,6,7,8-hexahydroquinoline-3-carboxylate*⁸

Yellow solid, M.P.: 224–226 °C, IR (KBr) ν (cm^{-1}): 3274 (N-H stretch), 3075 (C-H, aromatic), 2958–2933 (C-H, aliphatic), 1702 (C=O ester), 1604 (C=O ketone), 1491 (C=C, aromatic), 1280 (C-O, ether), 1072 (C-Br). ^1H NMR (400 MHz, $\text{DMSO}-d_6$): δ (ppm) = 0.86 (s, 3 H, CH_3), 1.01 (s, 3 H, CH_3), 1.13 (t, 3 H, $\text{O}-\text{CH}_2-\text{CH}_3$), 2.02 (d, 1H, CH), 2.21 (d, 1H, CH), 2.28 (m, 1H, CH), 2.30 (s, 3 H, CH_3), 2.41 (d, 1H, CH), 3.38 (s, 1H), 3.98 (q, 2 H, $\text{O}-\text{CH}_2-\text{CH}_3$), 4.84 (s, 1H, CH), 7.17 (d, 2 H, Ar-H), 7.30 (m, 1H), 9.17 (s, 1H, NH). ^{13}C NMR (100 MHz, $\text{DMSO}-d_6$): δ (ppm) 14.55, 183.80, 26.82, 29.56, 32.64, 36.55, 39.85, 50.58, 59.62, 103.43, 109.88, 121.46, 126.99, 129, 130.57, 130.84, 146.05, 150.3, 150.7, 167.01, 194.73.

Antibacterial activity

To assess the antibacterial properties of the synthesized nanocomposite, four microorganisms were prepared as lyophilized powders: *E. coli* (ATCC 11700), *S. aureus* (ATCC 25923), *S. typhi* (ATCC 13311), and *E. faecalis* (ATCC 25922). Isolates of MRSA and VRE were obtained from the pediatric intensive care unit (PICU) of Namazi Hospital in Shiraz, Iran. These isolates were initially assessed for resistance prior to undergoing antimicrobial susceptibility testing.

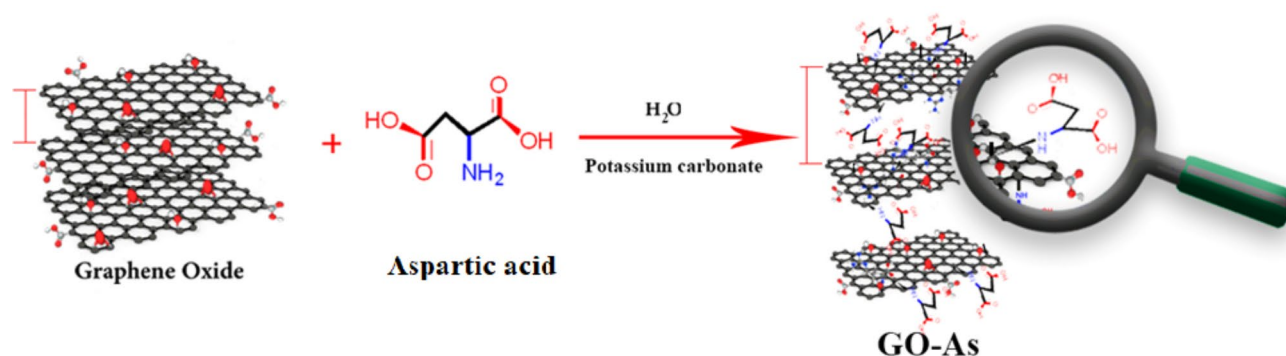


Fig. 1. Preparation of bifunctional organocatalyst.

The antimicrobial efficacy of As, GO, and GO-As was assessed against selected bacterial strains utilizing the broth microdilution technique, in accordance with the Clinical and Laboratory Standards Institute (CLSI) guidelines (CLSI M07, 2019). The bacterial strains were first cultivated on Mueller-Hinton agar (MHA) and incubated at 37 °C for a duration of 18 to 24 h to ensure optimal growth. Following the incubation period, a bacterial suspension was prepared in sterile saline (0.85% NaCl) and adjusted to turbidity corresponding to the 0.5 McFarland standard (approximately $1-2 \times 10^8$ CFU/mL) utilizing a densitometer or by visual comparison with the McFarland standard.

To establish the minimum inhibitory concentration (MIC), a two-fold serial dilution of each substance (As, GO, and GO-As) was performed in Mueller-Hinton broth (MHB). The concentrations tested ranged from 500 µg/mL to 1 µg/mL (500, 250, 100, 50, 25, 10, 5, and 1 µg/mL). A 96-well microtiter plate was employed for this assay, with each well containing 100 µL of the diluted compound and 100 µL of the bacterial suspension, resulting in a final inoculum concentration of 5×10^5 CFU/mL. Each plate incorporated positive controls (MHB with bacterial inoculum but without the compound) and negative controls (MHB with the compound but without bacterial inoculum) to ensure the validity of the assay.

The plates were incubated at a temperature of 37 °C for a duration of 16 to 20 h under aerobic conditions. Following the incubation period, the minimum inhibitory concentration (MIC) was assessed as the lowest concentration of the compound that achieved complete inhibition of visible bacterial growth, evidenced by the absence of turbidity in the wells. The results were validated through visual inspection, and, when necessary, by utilizing a microplate reader to measure the optical density at 600 nm (OD_{600}).

Results and discussion

The targeted biocatalyst was synthesized through a two-step process. Initially, GO was generated from natural graphene powder, in accordance with methodologies outlined in previous studies³⁹. In the subsequent step, aspartic acid was rapidly conjugated to the surface of the graphene oxide in an aqueous solution, adhering to environmentally sustainable conditions. This method eliminated the need for toxic substances and hazardous activators, facilitated the reaction at ambient temperature, and employed green solvents. These elements are critical for the effective binding of amino acids to GO, as emphasized in this investigation. The resulting composite exhibits amino acids uniformly arranged and covalently bonded to the surface of GO, thereby establishing spacing between the layers. This composite serves as a practical, reusable, and environmentally friendly catalyst. Following the synthesis of the desired composite, characterization was conducted utilizing FT-IR, SEM, EDX, mapping, and XRD analyses.

FTIR analysis

FTIR analysis of As (a), GO (b), and GO-As (c) is given in Fig. 2, and the comparison of these three spectra shows the formation of the desired composite. The FT-IR spectrum of the amino acid Aspartic (a) displays several peaks with varying intensities spectrum. The peak at 3171 cm^{-1} corresponds to NH group stretching. The -COO vibration is observed at 1607 cm^{-1} . The peaks at 2962 cm^{-1} , 2087 cm^{-1} , 1680 cm^{-1} , 1421 cm^{-1} , and 1150 cm^{-1} correspond to C-H group stretching, C=O vibration, COO^- vibration, and C-NH₂ vibration^{40,41}.

The stretching vibration of the OH groups on the graphene sheet and carboxylic wall is responsible for the broad peak in the graphene oxide spectrum in region 3280 (b). This peak moves to region 3481 when Aspartic acid functionalizes it (c). The stretching vibrations of C=O and C=C groups of graphene oxide are represented by the two peaks in the (b) spectrum, located in areas of 1731 and 1592 cm^{-1} , respectively. The 1347 and 1225 cm^{-1} regions likewise show peaks associated with the C-O groups of epoxy and alkoxide, respectively⁴². Placing As on the GO sheets results in noticeable spectral changes, including the removal, displacement, and formation of peaks (Fig. 2. c). C=O stretching groups of amide and carboxylate salt were detected at $1592-1680$. The OH and NH stretching groups were also shown to the peaks at 3481. The peak seen at 2982 is attributed to CH₃, which indicates that a bond has been formed between the amino acid and the functional groups found in graphene oxide.

EDX analysis

Using EDX analysis, the elements present in the composite were identified (Fig. 3). The presence of N in this analysis confirms the presence of amino acids in the composite. Additionally, the weight percentages of C, N, and O were 52.03, 8.96, and 39.00, respectively, indicating the existence of aspartic acids in the catalyst's structure. Next, the placement of elements in the composite was investigated. EDX-mapping analysis (Fig. 3) confirmed the elements' uniform distribution.

FE-SEM analysis

The morphology of graphene oxide and graphene oxide-aspartic acid was investigated using FE-SEM analysis (Fig. 4a-d). The comparison of these two analyses shows the difference in the morphology of graphene oxide after functionalization. The presence of aspartic acid on the surface of graphene oxide-aspartic acid is a good confirmation of the changes made on the surface of graphene oxide after the stabilization of amino acid on its surface. Moreover, SEM analysis was used to detect morphological changes in the samples.

XRD analysis

In Fig. 5, the XRD analysis of GO and functionalized GO (FGO) is presented. This analysis allows us to determine the distance between the layers of graphene oxide. As noted, the introduction of aspartic acid onto the surface of graphene oxide leads to an increased interlayer distance. Significant dispersion peaks are observed for graphene oxide at $2\theta = 11.4^\circ$, and for functionalized graphene oxide at $2\theta = 10.67^\circ$. While GO exhibits an inter-structural

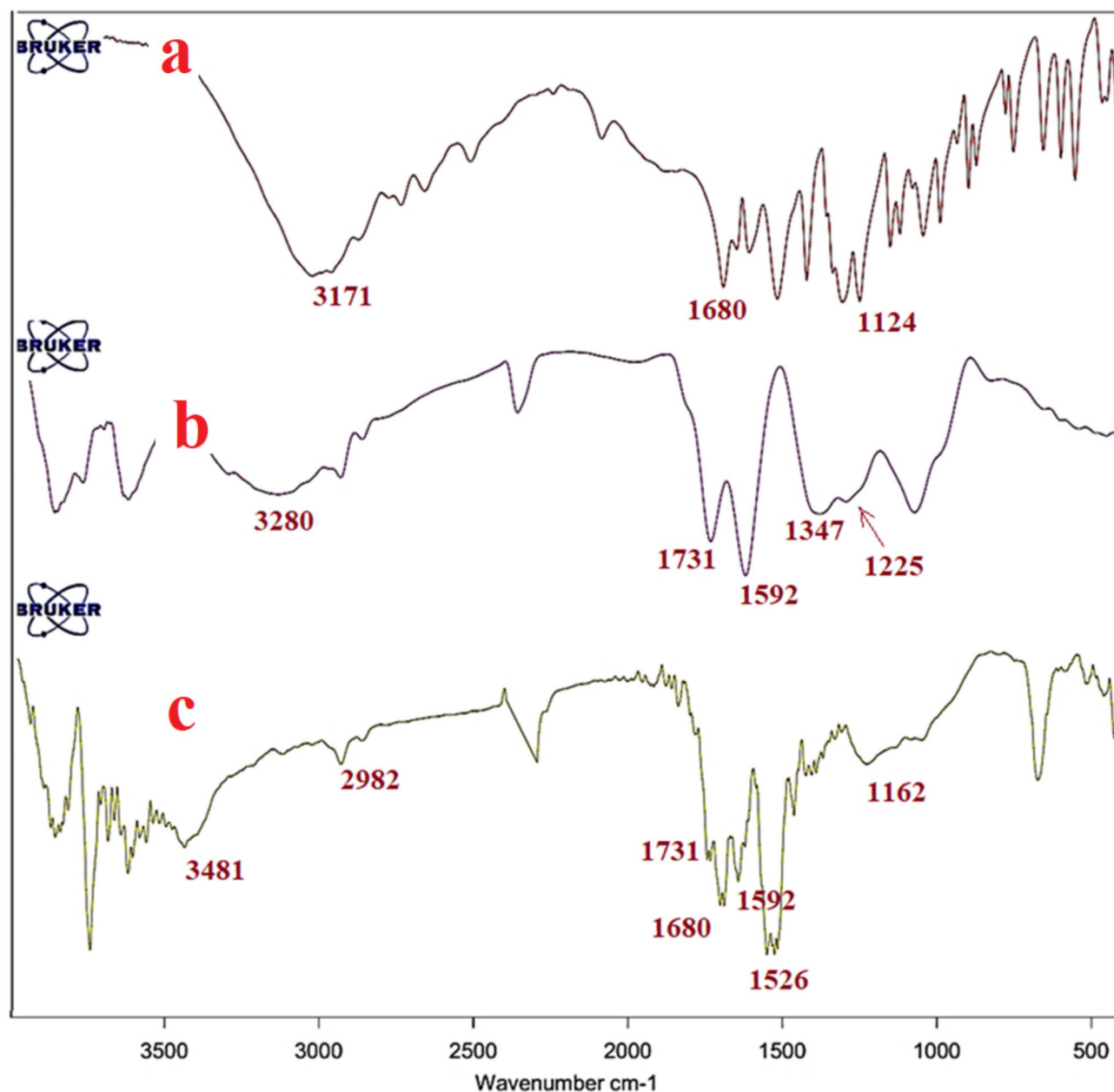


Fig. 2. FTIR analysis of (a) Aspartic acid, (b) GO, and (c) GO-AS.

distance of 0.389 nm (at $2\theta = 11.4^\circ$), the modification with aspartic acid increases this distance to 0.423 nm (at $2\theta = 10.67^\circ$) in the composite. According to the XRD results, aspartic acid is located between the layers of GO.

Raman analysis

Raman spectroscopy is a powerful technique for analyzing carbon structures, making it a valuable tool for investigating the structural modifications of graphene oxide after its functionalization with aspartic acid (see Fig. 6). The Raman spectrum of graphene oxide typically shows two prominent peaks, known as the D and G bands, which are associated with sp^3 and sp^2 carbon atoms, respectively. Therefore, the intensity ratio of the G band to the D band (I_D/I_G) is a crucial metric for evaluating the relative proportions of sp^2 and sp^3 carbon regions.

GO displays a G band at 1579.23 cm^{-1} and a D band at 1346 cm^{-1} . After functionalization, the G and D bands of graphene oxide shift to 1588 cm^{-1} and 1348.79 cm^{-1} , respectively, and there is an increase in the intensity of the D band. The increased I_D/I_G ratio of functionalized graphene oxide (1.03) compared to that of GO (1.01) indicates the incorporation of sp^3 hybridization into the graphene oxide sheets.

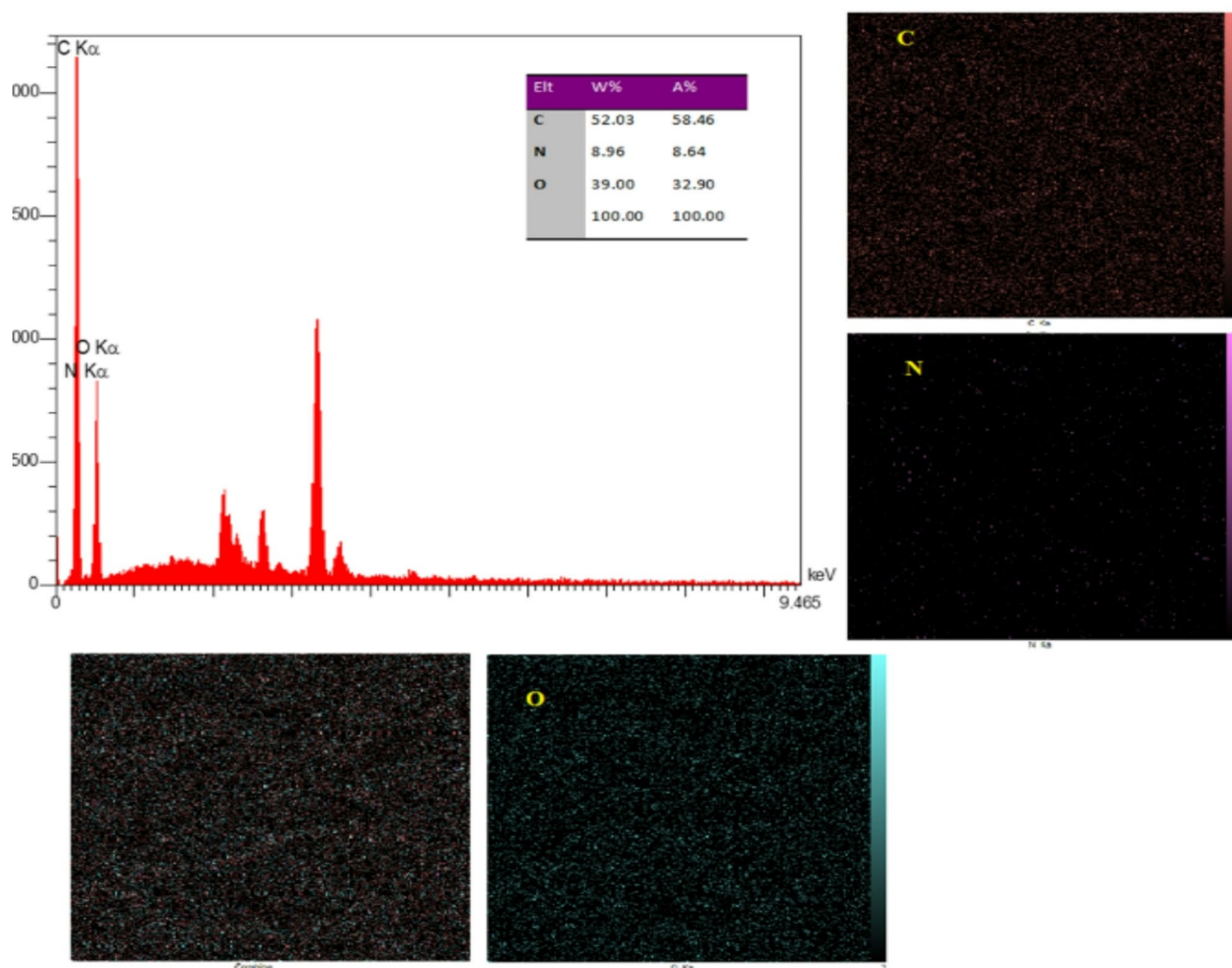


Fig. 3. EDX and EDX-mapping GO-As.

TGA analysis

Thermogravimetric analysis (TGA) is a valuable technique for quantifying the amount of amino acids bonded to the catalyst (see Fig. 7). Between 150 and 600 °C, the covalent bonds between the amino acids and graphene oxide (GO) layers begin to break down. In the TGA analysis of GO-As, an initial weight loss occurs at temperatures ranging from 80 to 100 °C, which is associated with the evaporation of water molecules. The second phase of degradation happens at around 200 °C and is attributed to the removal of oxygen-containing functional groups, resulting in the release of CO₂, CO, and water vapor. After this decomposition, the residual mass is recorded at 33.74%.

Ultimately, a final residual weight of 77% remains after a weight loss of approximately 20%. This weight loss can be explained by the thermal breakdown of organic groups on the GO surface. These results confirm that aspartic acid molecules have successfully adhered to the GO sheets. The chemical linkages formed by aspartic acid enhance the pyrolysis resistance of the functionalized GO.

Optimizing the reaction conditions for synthesis of polyhydroquinoline

Following the preparation and identification of graphene oxide (GO-As), the catalytic activity of the desired composite was investigated for the synthesis of polyhydroquinolines. In this study, 4-nitrobenzaldehyde, dimedone, ammonium acetate, and ethyl acetoacetate were chosen as the model reaction to optimize the conditions. The reaction was examined under various temperature conditions, solvents, and catalyst amounts. The results of these experiments are provided in Table 1.

To assess the effect of amino acids and to confirm their binding to the surface of graphene oxide, the reaction was conducted under three different conditions: with graphene oxide alone, with graphene oxide combined with aspartic acid, and without any catalyst (see Table 1, entries 1–3). Graphene oxide possesses acidic properties due to the presence of carboxylic acid groups, which enables it to catalyze the reaction to some extent. Aspartic acid, containing both carboxylic acid and amino groups, can function as both an acid and a base within the reaction.

The presence of aspartic acid on the surface of graphene oxide establishes it as a bifunctional catalyst. The results shown in Table 1, entry 3, confirm this assertion. The binding of aspartic acid to graphene oxide enhances

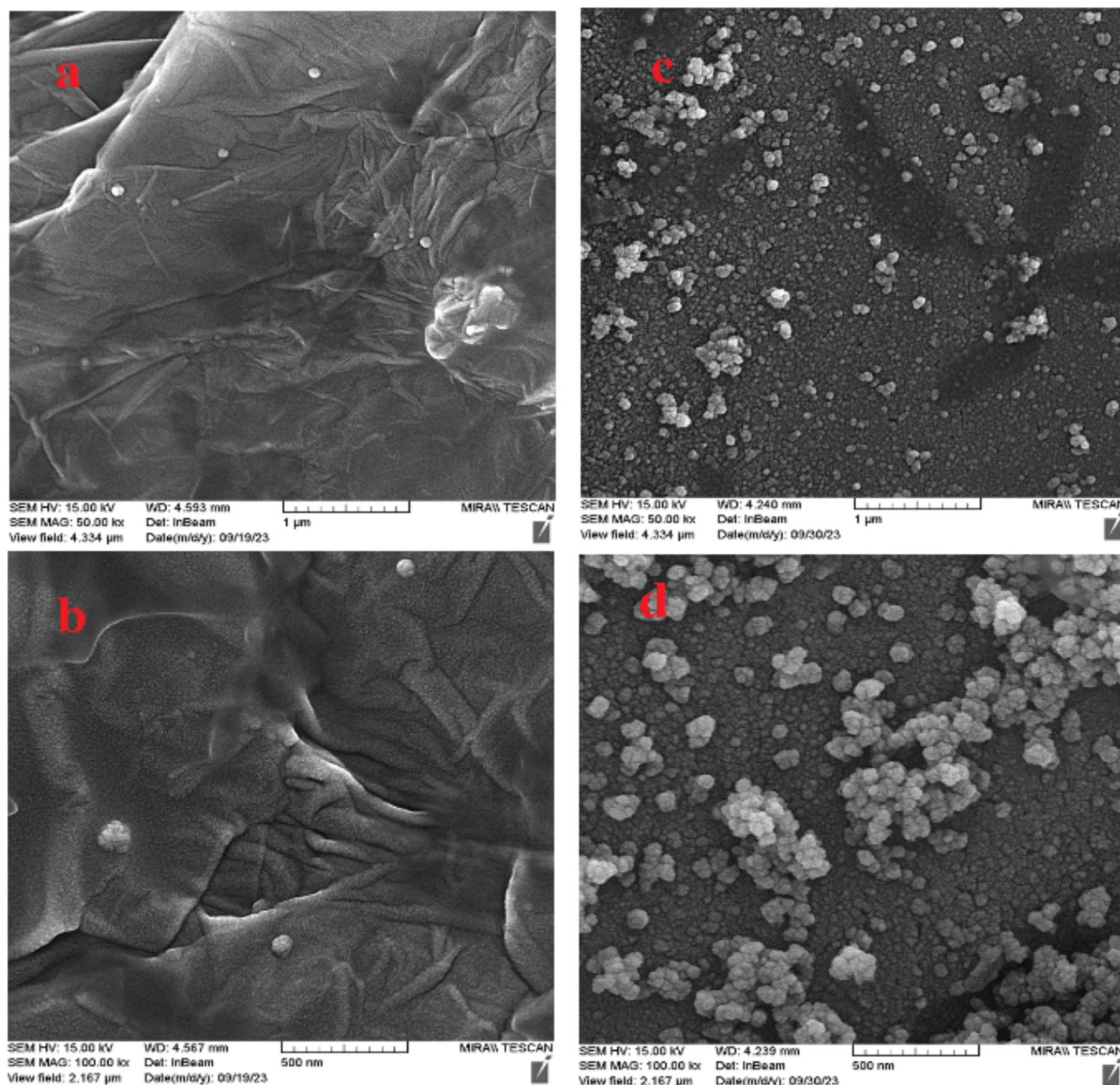


Fig. 4. FE-SEM images of GO (a,b) and GO-As (c,d).

the catalytic process and increases the reaction efficiency, leading to quicker results due to the accumulation of the catalyst.

Next, we optimized the reaction at different temperatures. The model reaction was conducted at room temperature and at 70 °C, with the latter being identified as the optimal temperature (see Table 1, entries 3–4).

We also investigated the model reaction under various solvent conditions: solvent-free, in H₂O, in a mixture of H₂O and EtOH (1:1), and in EtOH alone, to determine the best solvent for the reaction. Water, known for being a harmless, accessible, low-risk, and eco-friendly solvent, often faces the challenge of dissolving organic compounds. This issue was addressed by using ethanol in combination with water. The results indicated that the H₂O/EtOH solvent mixture produced the most favorable outcomes (refer to Table 1, entries 5–7).

Additionally, we tested the model reaction using varying amounts of the desired catalyst (0.02 g, 0.03 g, and 0.04 g). The highest yield was achieved with a 0.03 g catalyst (as shown in Table 1, entries 7–9).

Finally, the optimal results were obtained by conducting the reaction in an H₂O/EtOH (1:1) solvent with 0.03 g of catalyst at 70 °C, as recorded in Table 1, entry 8.

After establishing the optimal conditions, various polyhydroquinoline derivatives were synthesized, and the results are reported in Table 2.

A comparison of previous works is outlined in Table 3 to demonstrate the effectiveness of our current research on the synthesis of PHQs. The results indicate that our method operates under milder and more favorable

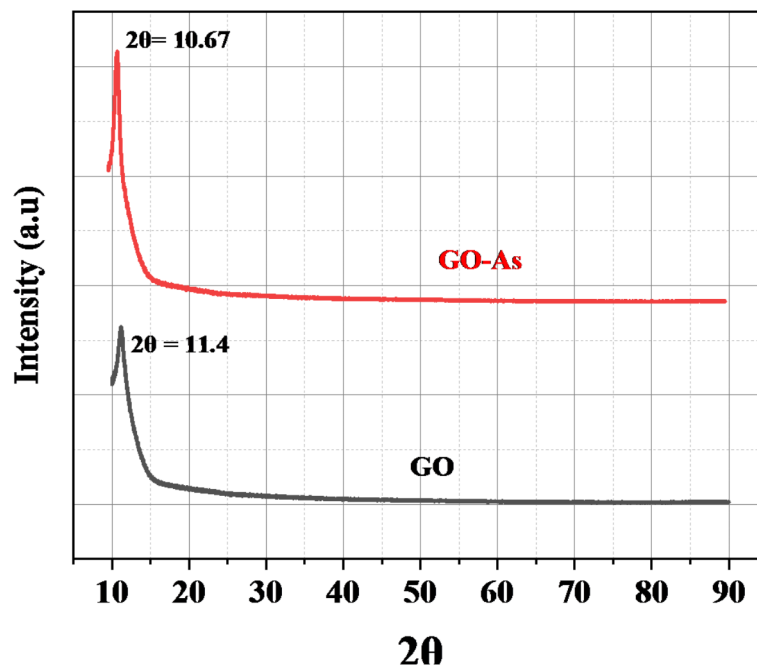


Fig. 5. XRD patterns of GO and GO-As.

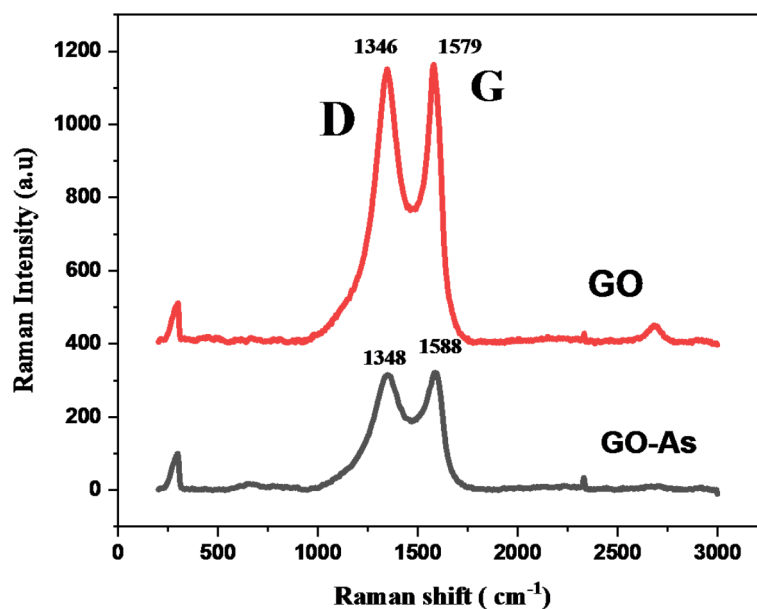


Fig. 6. Raman spectroscopy of GO and GO-As.

conditions, utilizing a bifunctional catalyst that possesses both acidic and basic properties. This advantage can be attributed to the preparation methods of various other catalysts, where metal is often coordinated to the surface. After use, this metal can detach from the catalyst's surface, leading to potential contamination of the reaction environment. In contrast, our catalyst is designed with an organic compound that is firmly attached to the substrate through strong covalent bonds, ensuring that its structure remains unchanged even after multiple uses.

The synthesis of polyhydroquinolines employing amino acid-functionalized graphene oxide (GO-As) as a dual acid-base catalyst adheres to a well-defined mechanism that is substantiated by existing literature^{43,45}. The carboxylic acid groups ($-\text{COOH}$) present on GO-As activate the carbonyl group of the aldehyde, thereby augmenting its electrophilicity. Concurrently, the basic amino groups ($-\text{NH}_2$) facilitate the enolization of dimedone (see Fig. 8). The enol form of dimedone subsequently undergoes a Knoevenagel condensation with the activated aldehyde, yielding Intermediate I, an α,β -unsaturated carbonyl compound. This reaction is pivotal for initiating the subsequent transformations that lead to the final product.

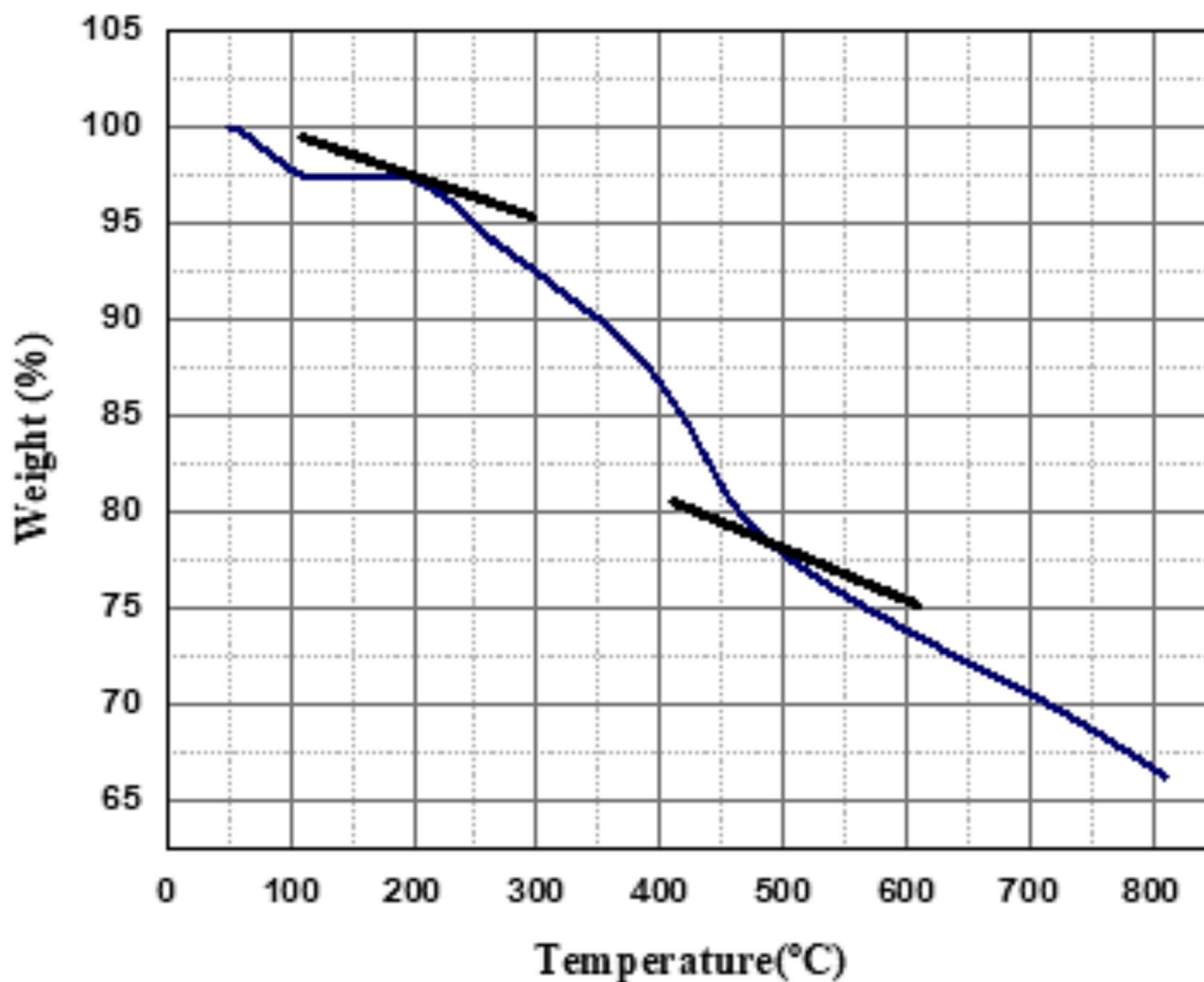
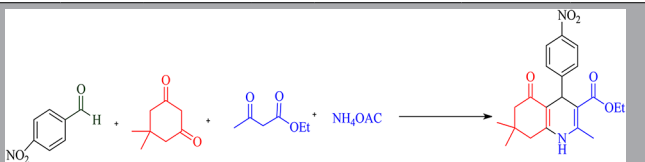
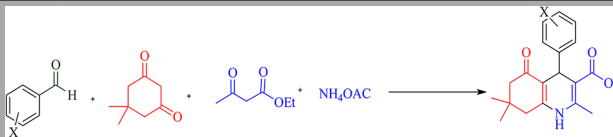
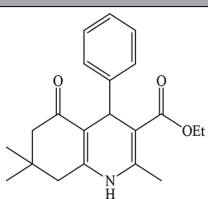
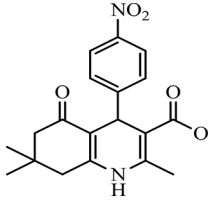
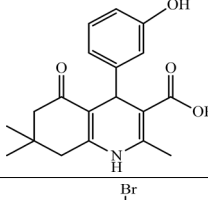
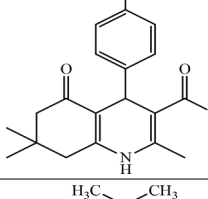
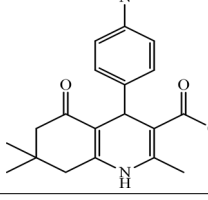
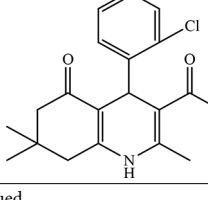


Fig. 7. Thermal gravimetric analysis of GO-As.



Entry	Catalyst	Catalyst (g)	Temp	Solvent	Time (min)	Yield ^b (%)
1	–	–	70	EtOH	70	51
2	GO	0.04	70	EtOH	70	51
3	GO-As	0.04	70	EtOH	12	95
4	GO-As	0.04	r.t.	EtOH	25	65
5	GO-As	0.04	70	EtOH/H ₂ O (1:1)	12	95
6	GO-As	0.04	70	Sovent-free	15	95
7	GO-As	0.04	70	H ₂ O	50	65
8	GO-As	0.03	70	EtOH/H ₂ O (1:1)	12	95
9	GO-As	0.02	70	EtOH/H ₂ O (1:1)	30	82

Table 1. Optimization of reaction conditions^a. ^aReaction conditions 1a: 4-nitrobenzaldehyde (0.151 g, 1 mmol), dimedone (0.14 g, 1 mmol), ammonium acetate (0.115 g, 1 mmol), ethyl acetoacetate (0.13 g, 1 mmol), and GO-As as catalyst. ^bIsolated yield.

				
Entry	Product	Time (min)	Yield (%) ^b	m. p. (ref.)
1		17	90	205–206 ⁴³
2		12	95	236–240 ⁴⁴
3		20	91	208–209 ⁴⁵
4		10	95	252–256 ⁴⁴
5		15	95	232–234 ⁴⁶
6		12	91	208–212 ⁴⁴
Continued				

Entry	Product	Time (min)	Yield (%) ^b	m. p. (ref.)
7		17	91	260–261 ⁴⁷
8		15	95	224–226 ⁴⁸

Table 2. GO-As (0.03 g) catalyzed multicomponent reactions for the one-pot efficient synthesis of polyhydroquinoline derivatives.

Entry	Catalyst/Temp/Time/Solvent	Yield (%)	Ref.
1	Ru ^{III} @CMC/Fe ₃ O ₄ / 80 °C / 20 min / Solvent-free	92	⁴⁹
2	SBA-15@AMPD-Co / 100 °C/35 min / Solvent-free	97	⁵⁰
3	Fe ₃ O ₄ @SiO ₂ @BHA-Cu(II)/ 50 °C/ 15 min / EtOH	97	⁵¹
4	PMO-ICS-PrSO ₃ H/reflux/20 min /EtOH	95	⁵²
5	Fe ₂ O ₃ @NH ₂ -SiO ₂ @Co(II)/ Reflux / 14 min / EtOH	95	⁵³
6	GO-As/ 70°C/12 min/ H ₂ O: EtOH(1:1)	95	This work

Table 3. Comparison of the efficiency of GO-As and other catalysts reported for synthesizing polyhydroquinolines.

Subsequent to this, the β -ketoester is activated by the acidic sites of GO-As, thereby enhancing its reactivity towards nucleophilic attack. Ammonium acetate (NH₄OAc) serves as a source of ammonia (NH₃), which reacts with the β -ketoester to generate Intermediate II. The basic sites of the catalyst abstract a proton from the β -ketoester, resulting in the formation of an enolate that acts as a nucleophile. This enolate then undergoes a Michael addition to the α,β -unsaturated carbonyl group of Intermediate I, a process facilitated by the dual acid-base characteristics of the catalyst. The result of this reaction is Intermediate III, a critical precursor to the final product.

The concluding step entails the intramolecular cyclization of Intermediate III, which is facilitated by the nucleophilic attack of the amine group on the carbonyl carbon. This cyclization eliminates water and culminates in the formation of the polyhydroquinoline product. The dual acid-base sites of GO-As are pivotal in stabilizing the transition state and promoting the removal of water, thereby ensuring high yield and selectivity.

The distinct architecture of GO-As, characterized by the presence of both acidic (–COOH) and basic (–NH₂) sites, enables it to act as a bifunctional catalyst. The acidic sites activate electrophiles such as aldehydes and β -ketoesters, while the basic sites generate nucleophiles, including enols and enolates. This synergistic interplay enhances the efficiency of the reaction, allowing it to proceed under mild and environmentally friendly conditions. The proposed mechanism illustrates the versatility and efficacy of GO-As as a dual acid-base catalyst for the sustainable synthesis of polyhydroquinolines. By exploiting its bifunctional properties, GO-As facilitates a series of reactions encompassing aldehyde activation, enolization, Knoevenagel condensation, Michael addition, and cyclization, ultimately yielding the desired product. This mechanism underscores the potential of GO-As as a sustainable and reusable catalyst for organic transformations.

The green synthesis of polyhydroquinolines utilizing graphene oxide-aspartic (GO-As) as a catalyst offers several advantages compared to traditional methodologies. Primarily, the employment of GO-As as a bifunctional catalyst negates the necessity for toxic or expensive metal-based catalysts, thereby mitigating environmental and health risks. The dual acid-base properties of this catalyst facilitate the efficient activation of both electrophiles and nucleophiles, allowing for the reaction to occur under mild conditions while achieving

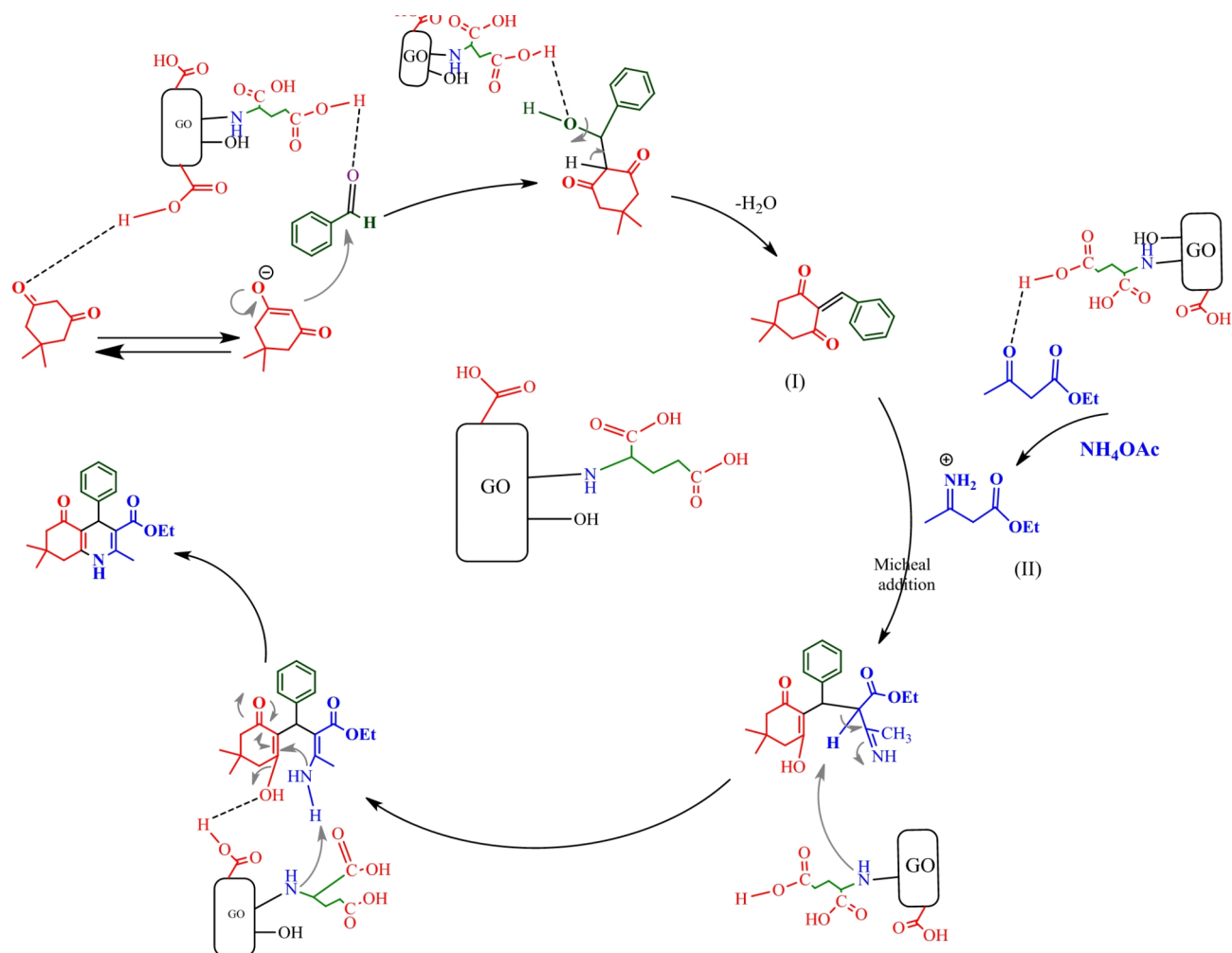


Fig. 8. Suggested mechanism for GO-As catalyzed one-pot synthesis of polyhydroquinoline.

high yield and selectivity. Furthermore, GO-As is reusable and can be easily recovered, which significantly reduces waste and enhances the overall process's sustainability. This method's absence of harsh reagents or solvents is consistent with the principles of green chemistry, rendering it both environmentally friendly and cost-effective. Another noteworthy advantage of this approach is its versatility and scalability. The synthesis can be performed under either solvent-free or aqueous conditions, which diminishes reliance on organic solvents and simplifies subsequent purification steps. The utilization of GO-As ensures that the final product is devoid of metal contamination, a crucial consideration in pharmaceutical applications. Additionally, the mild reaction conditions combined with the high efficiency of the catalyst make this method suitable for large-scale industrial implementation. By integrating sustainability, efficiency, and practicality, this green synthesis marks a significant advancement in the domains of organic synthesis and catalysis.

Reusability of the catalyst

One of the features of green catalysts is their capability to be reused. For this reason, this characteristic was investigated for the GO-As catalyst (Fig. 9). After performing the model reaction, and the catalyst was separated, washed with hot ethanol several times, and dried overnight at room temperature. Then, it was reused in the model reaction 6 times, and the results showed that the yield and reaction time did not change significantly. As a result, the catalyst can be reused many times without much change in the catalytic activity. The IR comparison of the original catalyst with the washed catalyst (after 1st run) is given in Fig. 10.

Antibacterial activity

The antibacterial behavior of GO, Aspartic acid, and GO-Aspartic acid against Gram-positive bacterial strains (*S. aureus* and *E. faecalis*), Gram-negative strains (*E. coli* and *S. typhi*), and two Gram-positive antibiotic-resistant bacteria (MRSA and VRE) were evaluated by dilution method.

Figure 11 shows the viability percentage of bacteria species exposed to different concentrations of three compounds, which exhibit a concentration-dependent antibacterial effect. The MIC values obtained are given in Table 4.

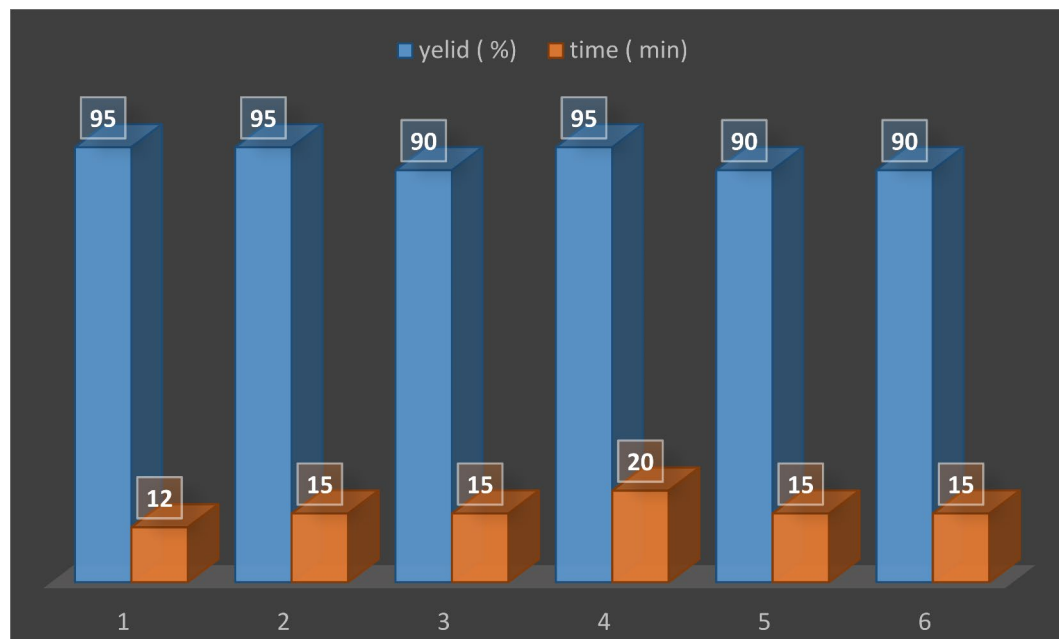


Fig. 9. Catalyst recycling experiment of GO-As in synthesis of 1a.

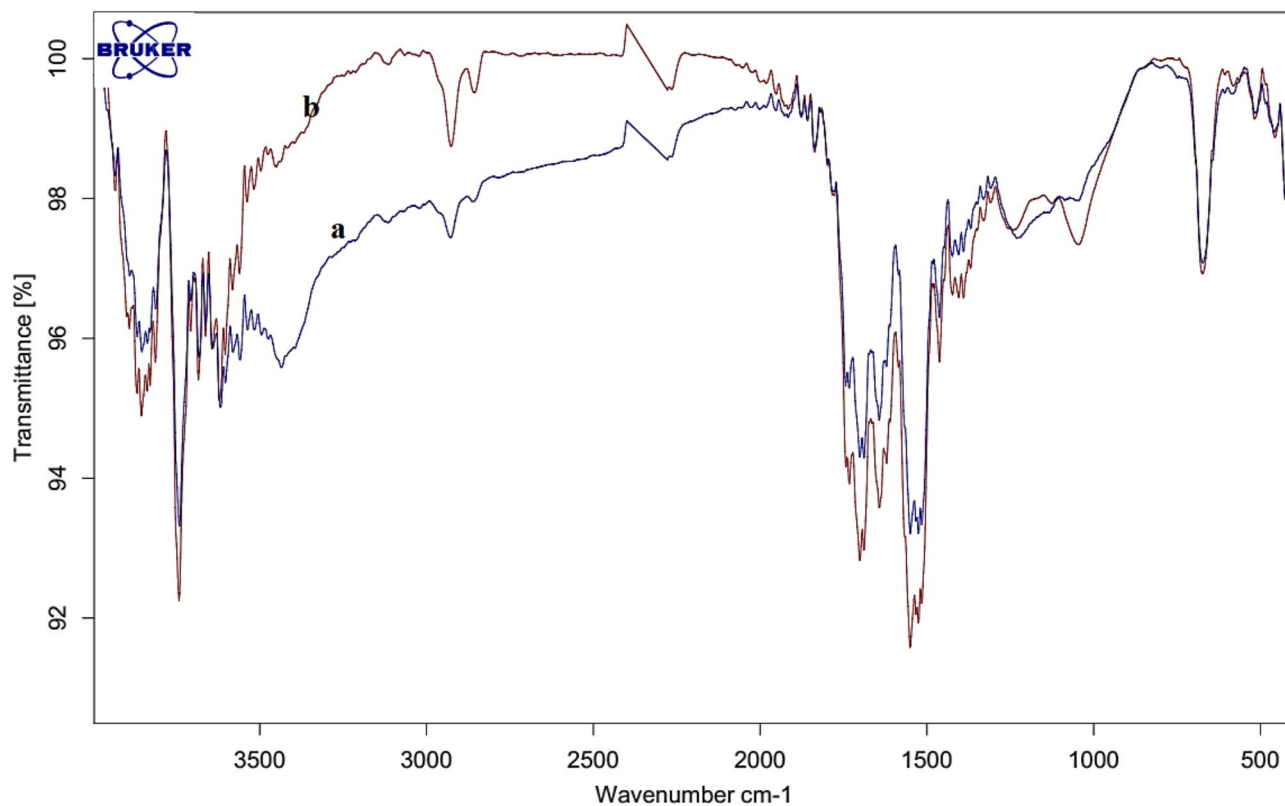


Fig. 10. FT-IR spectrum of GO-As before (a) and after 1st run (b).

In 2010, the antibacterial property of GO nanosheets was reported for the first time⁵⁴. After that, it was investigated in several other studies^{55–57}, which all indicated the antibacterial activity of GO. Also, in this study, the results for the antibacterial effect of GO were consistent with those of previous studies. They revealed that GO was effective against gram-positive and gram-negative bacteria (Fig. 9; Table 4.). Various factors, including oxidative stress, entrapment, and membrane stress, explain the antibacterial properties of GO. The sharp edges



Fig. 11. The viability percentage of 6 bacteria species, *S. aureus*, *E. faecalis*, *E. coli*, *S. typhi*, MRSA, and VRE, were exposed to different concentrations of as, GO, and GO-As.

of GO sheets can damage bacterial membranes and lead to the loss of bacterial activity^{58–60}. Also, oxygen free radicals produced by GO can lead to bacterial DNA damage and mitochondrial dysfunction^{61,62}.

We also investigated the antibacterial efficiency of pure aspartic acid, which had little effect on all tested bacteria species according to the results. However, based on the MIC result, when GO was functionalized with aspartic acid, its antibacterial activity increased 2 to 10 times against different bacteria (Table 4.). When aspartic acid bonds to the surface of GO, the number of carboxylic acid groups on that structure increases, which can

	Compound	<i>E. coli</i>	<i>S. typhi</i>	<i>S. aureus</i>	<i>E. faecalis</i>	MRSA	VRE
1	As	> 500	> 500	> 500	> 500	> 500	> 500
2	GO	500	250	100	250	500	500
3	GO-As	250	100	10	50	250	250

Table 4. The MIC values of as, GO, and GO-As toward microbial strains.

enhance GO-As's antimicrobial properties compared to GO. Also, according to the results, GO-As was more effective against gram-positive bacteria like *S. aureus* and *E. faecalis* than Gram-negative species like *E. coli* and *S. typhi* with the MIC value of 10 µg/mL and 50 µg/mL relative to 250 µg/mL and 100 µg/mL. This could be because gram-positive bacteria have a thick outer layer of peptidoglycan. There is a high tendency for the interaction of the negative surface charge of GO-As and the positively charged bacterial cell wall. In contrast, Gram-negative bacteria have two cell membranes (inner and outer membrane), and the peptidoglycan layer is sandwiched between the two layers. The cell walls of gram-negative bacteria are surrounded by a lipopolysaccharide (LPS) layer that prevents entry into the cell^{63,64}.

Also, this research investigated the effect of the three mentioned compounds on two resistant bacteria (MRSA and VRE). According to the results, this nanocomposite had a bacteriostatic effect against both pathogenic species, revealing the good antimicrobial potential of this compound. As seen in Table 4, the antibacterial property of GO was half of GO-As (MIC value of 500 µg/mL for GO relative to 250 µg/mL for GO-As).

Several studies have been conducted on the antibacterial properties of nanocomposite based on GO. For instance, in 2021, the antibacterial effect of GO/Cu₂O/ZnO nanocomposite was investigated, and it was reported that the antibacterial efficiency of nanocomposite increased compared to each of the compounds alone⁶⁵. In 2021, the antibacterial properties of amino-functionalized graphene oxide were investigated, and this compound was introduced as an antimicrobial agent⁶⁶. So far, the antibacterial effect of Go nanocomposite functionalized with amino acid has not been investigated. In this study, graphene oxide that has been modified by aspartic acid in a straightforward and green method was able to act effectively against microorganisms, even against two resistant bacteria, and reveals that this nanocomposite can be considered a novel antibacterial agent in biological fields. The antimicrobial efficacy of aspartic acid-loaded graphene oxide (GO-As) against multidrug-resistant pathogens, such as Methicillin-resistant *Staphylococcus aureus* (MRSA) and Vancomycin-resistant *Enterococcus* (VRE), is attributed to its distinctive physicochemical properties and multifaceted mechanisms of action. GO-As primarily exert their bactericidal effects through direct physical interactions and the induction of oxidative stress. The sharp edges and extensive surface area of GO-As enable them to function as “nanoknives,” penetrating bacterial membranes and inflicting physical damage, particularly to Gram-positive bacteria like MRSA and VRE, which lack the protective outer membrane present in Gram-negative organisms. Furthermore, GO-As can envelop bacterial cells, isolating them from their surroundings and disrupting nutrient uptake and membrane transport processes. These physical interactions are significantly augmented by generating reactive oxygen species (ROS), such as hydroxyl radicals and superoxide anions, inducing oxidative stress. ROS can impair essential cellular components, including lipids, proteins, and nucleic acids, leading to membrane degradation, enzyme inactivation, and damage to DNA and RNA. Ultimately, these effects result in bacterial cell death.

GO-As engages with bacterial biomolecules through π - π stacking and hydrogen bonding, which disrupts protein function and the structural integrity of nucleic acids. Its hydrophobic characteristics facilitate the extraction of phospholipids from bacterial membranes, destabilizing the lipid bilayer and compromising membrane integrity. Notably, the interaction between bacteria and GO-As can induce a “self-killing effect.” Bacterial metabolic activities reduce GO-As to rGO (reduced graphene oxide), which exhibits improved conductivity and hydrophobicity, exacerbating membrane damage and oxidative stress. This combination of physical disruption, oxidative stress, and biomolecular interactions establishes GO-As as a potent antimicrobial agent against multidrug-resistant pathogens.

Concisely, GO-As's dual acid-base functionality and distinctive structural properties enable it to effectively target MRSA and VRE through a synergistic approach involving both physical and chemical mechanisms. These findings highlight GO-As' potential as an innovative therapeutic agent for addressing antibiotic-resistant infections, particularly in clinical environments where conventional treatments may prove ineffective. Future research should prioritize the optimization of GO-As synthesis and application and evaluate its in vivo efficacy and safety for therapeutic purposes.

Conclusion

This study introduces a four-component synthesis of polyhydroquinolines utilizing an efficient heterogeneous biopolymeric organocatalyst. A notable aspect of this research is integrating an amino acid that binds effectively and economically to the surface of graphene oxide, resulting in a nanocomposite that exhibits dual acid-base properties. The synthesized composite displays commendable catalytic performance, and its role in synthesizing heterocyclic compounds has yielded satisfactory results. The covalent attachment of the amino acid to the graphene oxide surface significantly enhances the isolation and reusability of the catalyst, which constitutes a primary focus of this investigation. Furthermore, this methodology eliminates the necessity for toxic organic compounds, such as thionyl chloride, thus providing an additional benefit. The catalyst not only facilitates the efficient and rapid synthesis of polyhydroquinolines but also supports multiple reuses and the adoption of a green solvent. Future research may explore the potential of various amino acids with diverse structures.

The synthesized composite exhibits potential for additional applications, attributable to its distinct structural characteristics, thereby necessitating further investigation. This research also assessed the antibacterial efficacy of the synthesized nanocatalyst against six pathogenic bacterial species, with results substantiating its effectiveness. Notably, the antibacterial activity of the nanocomposite GO-As exceeds that of pure graphene oxide. Moreover, this approach provides a straightforward and efficient method for attaching various organic compounds to the surface of graphene oxide.

Data availability

All data generated or analyzed during this study are included in this published Article.

Received: 6 October 2024; Accepted: 13 March 2025

Published online: 25 March 2025

References

- Shirini, F. & Daneshvar, N. Introduction of taurine (2-aminoethanesulfonic acid) as a green bio-organic catalyst for the promotion of organic reactions under green conditions. *RSC Adv.* **6** (111), 110190–110205 (2016).
- Mahinroosta, M., Karimi, Z. & Allahverdi, A. Recycling of red mud for value-added applications: A comprehensive review. (2020).
- Amiri-Zirtol, L. & Gholami, A. Innovative synthesis of nano-magnetic bio-organocatalysts from red mud waste for green polyhydroquinoline derivatives synthesis. *Sci. Rep.* **14** (1), 26143 (2024).
- Tiwari, V. K., Kumar, A., Rajkhowa, S., Tripathi, G. & Singh, A. K. *Organocatalysis: a Versatile Tool for Asymmetric Green Organic Syntheses*. 261–315. (Introduction, Application and Scope: Springer, 2022).
- Amiri-Zirtol, L., Yargholi, A., Emami, L., Karimi, Z. & Khabnadideh, S. Preparation of a new reusable magnetic organocatalyst to synthesis of polyhydroquinoline derivatives as cytotoxic agents: synthesis and biological evaluation. *J. Saudi Chem. Soc.* **28** (6), 101922 (2024).
- Maleki, A., Firouzi-Haji, R. & Hajizadeh, Z. Magnetic guanidinylated Chitosan nanobiocomposite: a green catalyst for the synthesis of 1, 4-dihydropyridines. *Int. J. Biol. Macromol.* **116**, 320–326 (2018).
- Gholami, A. et al. Magnetic properties and antimicrobial effect of amino and Lipoamino acid coated iron oxide nanoparticles. *Minerva Biotechnologica* **28** (4), 177–186 (2016).
- Tiwari, J. et al. Organocatalytic mediated green approach: A versatile new L-valine promoted synthesis of diverse and densely functionalized 2-amino-3-cyano-4H-pyrans. *Synth. Commun.* **48** (2), 188–196 (2018).
- Amirnejat, S., Nosrati, A., Javanshir, S. & Naimi-Jamal, M. R. Superparamagnetic alginate-based nanocomposite modified by L-arginine: an eco-friendly bifunctional catalysts and an efficient antibacterial agent. *Int. J. Biol. Macromol.* **152**, 834–845 (2020).
- Amiri-Zirtol, L., Mostashfi, H., Sabet, R., Karimi, Z. & Ranjbar-Karimi, R. L-Aspartic acid-functionalized magnetic nanoparticles: as a new magnetically reusable [b]ifunctional acid-base catalysts for the synthesis of [b]enzo [b] Pyran and Pyrano [3, 2-c] Chromene derivatives. *Sci. Rep.* **15** (1), 248 (2025).
- Schafer, L. L. et al. *Applied Organometallic Chemistry: from Foundational To Translational*. 2377–2380. (ACS, 2024).
- Ameli, S., Davoodnia, A. & Pordel, M. Rapid one-pot aspartic acid-promoted synthesis of tetrahydrobenzo [b] Pyrans in water. *Org. Prep. Proced. Int.* **48** (4), 328–336 (2016).
- Ghorbani-Choghamarani, A., Hajjami, M., Gholamian, F. & Azadi, G. Aspartic acid as a highly efficient and nontoxic organocatalyst for the one-pot synthesis of tri- and tetrasubstituted imidazoles under solvent-free conditions. *Russ. J. Org. Chem.* **51**, 352–356 (2015).
- Ahad, A. & Farooqui, M. Organocatalyzed domino reactions: diversity oriented synthesis of pyran-annulated scaffolds using in situ-developed Benzyldenemalononitriles. *Res. Chem. Intermed.* **43**, 2445–2455 (2017).
- Hashemi, S. A. et al. Bio-enhanced polyrhodanine/graphene Oxide/Fe₃O₄ nanocomposite with Kombucha solvent supernatant as ultra-sensitive biosensor for detection of doxorubicin hydrochloride in biological fluids. *Mater. Chem. Phys.* **279**, 125743 (2022).
- Amiri-Zirtol, L. & Khabnadideh, S. A novel heterogeneous biocatalyst based on graphene oxide for synthesis of Pyran derivatives. *Sci. Rep.* **14** (1), 6957 (2024).
- Khabnadideh, S., Khorshidi, K. & Amiri-Zirtol, L. A novel heterogeneous acid-base nano-catalyst designed based on graphene oxide for synthesis of spiro-indoline-pyranochromene derivatives. *BMC Chem.* **17** (1), 12 (2023).
- Emadi, F., Emadi, A. & Gholami, A. A comprehensive insight towards pharmaceutical aspects of graphene nanosheets. *Curr. Pharm. Biotechnol.* **21** (11), 1016–1027 (2020).
- Golkar, N. et al. An oral nanoformulation of insulin: development and characterization of human insulin loaded graphene oxide-sodium alginate-gold nanocomposite in an animal model. *J. Drug Deliv. Sci. Technol.* **82**, 104309 (2023).
- Zhang, M., Liu, Y.-H., Shang, Z.-R., Hu, H.-C. & Zhang, Z.-H. Supported molybdenum on graphene oxide/Fe₃O₄: an efficient, magnetically separable catalyst for one-pot construction of spiro-oxindole dihydropyridines in deep eutectic solvent under microwave irradiation. *Catal. Commun.* **88**, 39–44 (2017).
- Chen, M.-N., Mo, L.-P., Cui, Z.-S. & Zhang, Z.-H. Magnetic nanocatalysts: synthesis and application in multicomponent reactions. *Curr. Opin. Green. Sustainable Chem.* **15**, 27–37 (2019).
- Zhang, M. et al. Catalyst-free, visible-light promoted one-pot synthesis of spirooxindole-pyran derivatives in aqueous Ethyl lactate. *ACS Sustain. Chem. Eng.* **5** (7), 6175–6182 (2017).
- Obaid, R. J. et al. Pharmacological significance of nitrogen-containing five and six-membered heterocyclic scaffolds as potent cholinesterase inhibitors for drug discovery. *Process Biochem.* **120**, 250–259 (2022).
- Mayurachayakul, P., Pluempunupat, W., Srisuwanakiet, C. & Chantarasriwong, O. Four-component synthesis of polyhydroquinolines under catalyst- and solvent-free conventional heating conditions: mechanistic studies. *RSC Adv.* **7** (89), 56764–56770 (2017).
- Kumar, P. et al. Palladium immobilized on functionalized Halloysite: A robust catalyst for ligand free Suzuki–Miyaura cross coupling and synthesis of Pyrano [2, 3-c] pyrazole motifs via four component cascade reaction and their in-silico antitubercular screening. *Appl. Catal. A* **689**, 120003 (2025).
- Shriya, S. B., Verma, S., Parothia, S., Angral, S. & Gupta, P. Immobilized SbCl₃@ Chitosan as a green heterogeneous catalyst for the synthesis of 1, 2, 4, 5-tetrasubstituted imidazoles. *Res. Chem. Intermed.* **50** (4), 1745–1755 (2024).
- Kumar, P. et al. Synthesis, biological evaluation, molecular Docking and kinetic investigation of new 2, 4, 5-Trisubstituted imidazole derivatives as antidiabetic agents. *ChemistrySelect* **8** (31), e202300924 (2023).
- Gupta, P., Kumar, P., Syal, B. & Shamim, T. Synthesis of 1, 4-disubstituted-1, 2, 3-triazoles using starch-functionalized copper (II) acetate as a recyclable heterogeneous catalyst in water. *Res. Chem. Intermed.* **48** (11), 4601–4615 (2022).
- Kumar, P., Gupta, P. & Sharma, C. Surface modified novel magnetically tuned Halloysite functionalized sulfonic acid: synthesis, characterization and catalytic activity. *Catal. Sci. Technol.* **11** (11), 3775–3786 (2021).
- Syal, B. & Gupta, P. Cobalt Single-Atom catalyst: synthesis, characterization and catalytic activity. *Applied organometallic chemistry*. *Applied organometallic chemistry*. *December* **38** (12), e7734 (2024).

31. Liao, H. Y., Kang, L. Q., Zhang, S. S. & Yan, J. H. Green synthesis of polyhydroquinolines catalyzed by silica-supported ionic liquid Si-[SbSipim][PF₆]. *J. Chin. Chem. Soc.* **66** (11), 1518–1522 (2019).
32. Zabihzadeh, M., Omid, A., Shirini, F., Tajik, H. & Langarudi, M. S. N. Introduction of an efficient DABCO-based bis-dicationic ionic salt catalyst for the synthesis of arylidenemalononitrile, Pyran and polyhydroquinoline derivatives. *J. Mol. Struct.* **1206**, 127730 (2020).
33. Sakram, B., Sonyanaik, B., Ashok, K. & Rambabu, S. Polyhydroquinolines: 1-sulfonylpyridinium chloride catalyzed an efficient one-pot multicomponent synthesis via Hantzsch condensation under solvent-free conditions. *Res. Chem. Intermed.* **42**, 7651–7658 (2016).
34. Dekamin, M. G. et al. Alginate: A mild and renewable bifunctional heterogeneous biopolymeric organocatalyst for efficient and facile synthesis of polyhydroquinolines. *Int. J. Biol. Macromol.* **108**, 1273–1280 (2018).
35. Eskandari, F., Abbaszadegan, A., Gholami, A. & Ghahramani, Y. The antimicrobial efficacy of graphene oxide, double antibiotic paste, and their combination against *Enterococcus faecalis* in the root Canal treatment. *BMC Oral Health* **23** (1), 20 (2023).
36. Nabavizadeh, M. et al. Chemical constituent and antimicrobial effect of essential oil from *Myrtus communis* leaves on microorganisms involved in persistent endodontic infection compared to two common endodontic irrigants: an in vitro study. *J. Conservative Dentistry Endodontics* **17** (5), 449–453 (2014).
37. Mousavi, S. M. et al. Recent breakthroughs in graphene quantum dot-enhanced sonodynamic and photodynamic therapy. *J. Mater. Chem. B* **12** (29), 7041–7062 (2024).
38. Gholami, A. et al. Expression of key apoptotic genes in hepatocellular carcinoma cell line treated with etoposide-loaded graphene oxide. *J. Drug Deliv. Sci. Technol.* **57**, 101725 (2020).
39. Amiri-Zirtol, L., Amrollahi, M. A. & Mirjalili, B.-F. GO-Fe₃O₄-Ti (IV) as an efficient magnetic catalyst for the synthesis of Bis (indolyl) methanes and benzo [a] xanthen-11-one derivatives. *Inorg. Nano-Metal Chem.* **53** (11), 1211–1221 (2023).
40. Wang, Z. et al. L-Aspartic acid capped cds quantum Dots as a high performance fluorescence assay for silver ions (I) detection. *Nanomaterials* **9** (8), 1165 (2019).
41. Mithil Kumar, N. et al. A novel biodegradable green Poly (l-aspartic acid-citric acid) copolymer for antimicrobial applications. *J. Polym. Environ.* **20**, 17–22 (2012).
42. Khabnadideh, S., Mirzaei, E. & Amiri-Zirtol, L. L-arginine modified graphene oxide: A novel heterogeneous catalyst for synthesis of [benzo [b] Pyrans and Pyrano [3, 2-c] Chromenes. *J. Mol. Struct.* **1261**, 132934 (2022).
43. Shakib, P., Dekamin, M. G., Valiey, E., Karami, S. & Dohendou, M. Ultrasound-promoted Preparation and application of novel bifunctional core/shell Fe₃O₄@ SiO₂@ PTS-APG as a robust catalyst in the expeditious synthesis of Hantzsch esters. *Sci. Rep.* **13** (1), 8016 (2023).
44. Kafshdarzadeh, K., Malmir, M., Amiri, Z. & Heravi, M. M. Ionic liquid-loaded triazine-based magnetic nanoparticles for promoting multicomponent reaction. *Sci. Rep.* **12** (1), 22261 (2022).
45. Farsi, R., Mohammadi, M. K. & Saghaneshad, S. J. Sulfonamide-functionalized covalent organic framework (COF-SO₃H): an efficient heterogeneous acidic catalyst for the one-pot Preparation of polyhydroquinoline and 1, 4-dihydropyridine derivatives. *Res. Chem. Intermed.* **47**, 1161–1179 (2021).
46. Ahankar, H., Ramazani, A. & Joo, S. W. Magnetic nickel ferrite nanoparticles as an efficient catalyst for the Preparation of polyhydroquinoline derivatives under microwave irradiation in solvent-free conditions. *Res. Chem. Intermed.* **42**, 2487–2500 (2016).
47. Mansoor, S. S., Aswin, K., Logaiya, K. & Sudhan, S. Bismuth nitrate as an efficient recyclable catalyst for the one-pot multi component synthesis of 1, 4-dihydropyridine derivatives through unsymmetrical Hantzsch reaction. *J. Saudi Chem. Soc.* **20**, S100–S8 (2016).
48. Shiri, L., Heidari, L. & Kazemi, M. Magnetic Fe₃O₄ nanoparticles supported imine/Thiophene-nickel (II) complex: A new and highly active heterogeneous catalyst for the synthesis of polyhydroquinolines and 2, 3-dihydroquinazoline-4 (1H)-ones. *Appl. Organomet. Chem.* **32** (1), e3943 (2018).
49. Chen, Y., Zhang, Z., Jiang, W., Zhang, M. & Li, Y. Ru III@ CMC/Fe₃O₄ hybrid: an efficient, magnetic, retrievable, self-organized nanocatalyst for green synthesis of Pyranopyrazole and polyhydroquinoline derivatives. *Mol. Diversity* **23**, 421–442 (2019).
50. Ghorbani-Choghamarani, A., Mohammadi, M., Tamoradi, T. & Ghadermazi, M. Covalent immobilization of Co complex on the surface of SBA-15: green, novel and efficient catalyst for the oxidation of sulfides and synthesis of polyhydroquinoline derivatives in green condition. *Polyhedron* **158**, 25–35 (2019).
51. Norouzi, M. & Beiranvand, S. Fe₃O₄@ SiO₂@ BHA-Cu (II) as a new, effective, and magnetically recoverable catalyst for the synthesis of polyhydroquinoline and tetrazole derivatives. *J. Chem. Sci.* **135** (3), 86 (2023).
52. Yaghoubi, A., Dekamin, M. G. & Karimi, B. Propylsulfonic acid-anchored isocyanurate-based periodic mesoporous Organosilica (PMO-ICS-PrSO₃H): A highly efficient and recoverable nanoporous catalyst for the one-pot synthesis of substituted polyhydroquinolines. *Catal. Lett.* **147**, 2656–2663 (2017).
53. Kouser, M., Chowhan, B., Sharma, N. & Gupta, M. Transformation of waste toner powder into valuable Fe₂O₃ nanoparticles for the Preparation of recyclable Co (II)-NH₂-SiO₂@ Fe₂O₃ and its applications in the synthesis of polyhydroquinoline and Quinazoline derivatives. *ACS Omega* **7** (51), 47619–47633 (2022).
54. Hu, W. et al. Graphene-based antibacterial paper. *ACS Nano* **4** (7), 4317–4323 (2010).
55. Bousiakou, L. G., Qindeel, R., Al-Dossary, O. M. & Kalkani, H. Synthesis and characterization of graphene oxide (GO) sheets for pathogen Inhibition: *Escherichia coli*, *Staphylococcus aureus* and *Pseudomonas aeruginosa*. *J. King Saud University-Science* **34** (4), 102002 (2022).
56. Aunkor, M. T. H. et al. Antibacterial activity of graphene oxide nanosheet against multidrug resistant superbugs isolated from infected patients. *Royal Soc. Open. Sci.* **7** (7), 200640 (2020).
57. Fallatah, H. et al. Antibacterial effect of graphene oxide (GO) nano-particles against *Pseudomonas Putida* biofilm of variable age. *Environ. Res. Pollut. Res.* **26**, 25057–25070 (2019).
58. Akhavan, O. & Ghaderi, E. Toxicity of graphene and graphene oxide nanowalls against bacteria. *ACS Nano* **4** (10), 5731–5736 (2010).
59. Li, X., Li, F., Gao, Z. & Fang, L. Toxicology of graphene oxide nanosheets against *paecilomyces Catenannulatus*. *Bull. Environ. Contam. Toxicol.* **95**, 25–30 (2015).
60. Liu, S. et al. Antibacterial activity of graphite, graphite oxide, graphene oxide, and reduced graphene oxide: membrane and oxidative stress. *ACS Nano* **5** (9), 6971–6980 (2011).
61. Pieper, H. et al. Toxizität von graphenoxid: endoperoxide Als ursache. *Angew. Chem.* **128** (1), 413–416 (2016).
62. Zhao, J., Wang, Z., White, J. C. & Xing, B. Graphene in the aquatic environment: adsorption, dispersion, toxicity and transformation. *Environ. Sci. Technol.* **48** (17), 9995–10009 (2014).
63. Sajjad, S. et al. GO/Ag₂O composite nanostructure as an effective antibacterial agent. *ChemistrySelect* **4** (35), 10365–10371 (2019).
64. Fisher, J. F. & Mobashery, S. Constructing and deconstructing the bacterial cell wall. *Protein Sci.* **29** (3), 629–646 (2020).
65. Li, L. et al. Arc erosion resistance of Al₂O₃-Cu/35Mo composites reinforced by trace graphene oxide. *J. Mater. Res. Technol.* (2024).
66. Lu, B.-Y. et al. Functionalized graphene oxide nanosheets with unique three-in-one properties for efficient and tunable antibacterial applications. *Nano Res.* **14** (1), 185–190 (2021).

Acknowledgements

Financial assistance from the Shiraz University of Medical Sciences by way of grant number 28542 is gratefully acknowledged.

Author contributions

Leila Amiri-Zirtol, Formal analysis, Writing – original draft. Hamideh Emtiazi, Methodology, Writing, Seyedeh Narjes Abootalebi, Review & editing. Ahmad Gholami, Supervision, Review & editing.

Declarations

Competing interests

The authors declare no competing interests.

Additional information

Supplementary Information The online version contains supplementary material available at <https://doi.org/10.1038/s41598-025-94389-0>.

Correspondence and requests for materials should be addressed to S.N.A. or A.G.

Reprints and permissions information is available at www.nature.com/reprints.

Publisher's note Springer Nature remains neutral with regard to jurisdictional claims in published maps and institutional affiliations.

Open Access This article is licensed under a Creative Commons Attribution-NonCommercial-NoDerivatives 4.0 International License, which permits any non-commercial use, sharing, distribution and reproduction in any medium or format, as long as you give appropriate credit to the original author(s) and the source, provide a link to the Creative Commons licence, and indicate if you modified the licensed material. You do not have permission under this licence to share adapted material derived from this article or parts of it. The images or other third party material in this article are included in the article's Creative Commons licence, unless indicated otherwise in a credit line to the material. If material is not included in the article's Creative Commons licence and your intended use is not permitted by statutory regulation or exceeds the permitted use, you will need to obtain permission directly from the copyright holder. To view a copy of this licence, visit <http://creativecommons.org/licenses/by-nc-nd/4.0/>.

© The Author(s) 2025